Trans. Phenom. Nano Micro Scales, 4(1): 1-10, Winter - Spring 2016
DOI: 10.7508/tpnms.2016.01.001

ORIGINAL RESEARCH PAPER

Conjugate Heat Transfer of MHD non-Darcy Mixed Convection Flow of a Nanofluid over a Vertical Slender Hollow Cylinder Embedded in Porous Media

B. Jafarian[1], M. Hajipour[2], R. Khademi[3,*]

[1]Department of Chemical Engineering, Persian Gulf University, 75168, Boushehr, I. R.Iran

[2]Faculty of Sciences, Science and Research Branch, Islamic Azad University, Tehran, I. R. Iran

[3]Department of Chemical Engineering, University of Sistan and Baluchestan, 98164-161, Zahedan, I. R.Iran

Received 17 July 2014; revised 29 October 2015; accepted 21 November 2015; available online 5 January 2016

ABSTRACT: In this paper, conjugate heat transfer of magneto hydrodynamic mixed convection of nanofluid about a vertical slender hollow cylinder embedded in a porous medium with high porosity have been numerically studied. The Forchheimer's modification of Darcy's law was used in representing the nanofluid motion inside the porous media. The governing boundary layer equations were transformed to non-dimensional differential equations by taking suitable similarity variables and solved numerically using differential quadrature method (DQM). The interfacial (solid-liquid) temperature distribution and the variations of velocity and temperature within boundary layer for different values of governing parameter in presence of uniform magnetic field have been presented and discussed. Our results demonstrate that heat transfer rate can enhance using nanofluid as well as porous medium, while magnetic field has no remarkable effect on the parameter. The computed results were also compared with those available in the existing literature and a good agreement was observed.

KEYWORDS: *Conjugate heat transfer; differential quadrature method (DQM); magneto hydrodynamic (MHD); MHD-mixed convection; nanofluid*

INTRODUCTION

When a solid body is placed in a clear fluid or in a porous medium different from solid temperature, conjugate (conduction-convection) heat transfer occurs. From an industrial and technological point of view, free, forced and mixed convection conjugate head transfer in porous media play significant roles in various engineering applications such as geothermal energy recovery, solar systems, crude oil extraction and flow through metal foams. These fundamental phenomena can be studied in several categories: laminar or turbulent, internal or external flow, vertical or horizontal and assisting or opposing flow based on the flow regime, geometry, orientation and sign of Grashof number, respectively. Nield and Bejan [1], Vafai [2, 3], Pop and Ingham [4], Ingham and Pop [5] and Vadasz [6] have done comprehensive studies of these interesting subjects mentioned above. Forced convection conjugate head transfer of micro-polar fluid flow along a vertical slender hollow circular cylinder was numerically studied by Chang [7].

He used the cubic spline collocation numerical method to solve the non-linear governing Equations. Further, Kaya [8] presented a numerical solution to investigate the magnetic field effect on mixed convection heat transfer about the vertical slender hollow cylinder by using the implicit finite difference method (Keller box). Then the researcher[9] solved this problem when the hollow cylinder is embedded in a porous medium with high porosity. He assumed the fluid was regular and in thermal equilibrium with the porous medium. However, regular fluid (such as water, oil and ethyl glycol), might not have enough thermal conductivity to provide desired efficiency. A good way to overcome this limitation is to disperse solid nanoparticles in the fluids.

It is worth mentioning nanoparticle with high contact surface causes to improve heat transfer ability and stability, while larger particle leads to several problems such as abrasion, clogging and pressure dropping. Numerous investigations have been done about the effect of nanoparticles on thermal performance. For example, Choi et al. [10] experimentally studied effective thermal conductivity of nanosolid-liquid mixture. Their results revealed that the dispersion of a small amount (<1% by volume) of carbon nanotubes in a liquid increases its thermal conductivity remarkably (nearly 200%).The principal aim of the present investigation is to extend the problem considered by Kaya [8] to the case in which the hollow cylinder is placed in saturated by porous media and water-based nanofluid and to solve governing equations using a new numerical method: differential quadrature method (DQM).

To show necessity and importance of the research area, some resent works as follow: Ahmad and Pop [11] reported a numerical study of mixed convection boundary layer flow from a vertical flat plate embedded in a porous medium filled with nanofluids.

*Corresponding Author Email: *ramin.khademi85@gmail.com*
Tel.: +987734823107

Nomenclature

B_0	magnetic field strength (T)
C_p	specific heat at constant pressure
$f(\eta)$	Similarity variable$\left(= Re_x^{1/2}(r^2 - r_o^2)/2r_o x\right)$
F	inertia coefficient of the porous medium (m^{-1})
F^*	Forchheimer parameter $(= Fr_0)$
G	acceleration due to gravity ($m\ s^{-2}$)
Gr	Grashofnumber $(= g\beta_f \Delta T\, l^3/\nu_f{}^2)$
K	thermal conductivity $[Wm^{-1}K^{-1}]$
Mn	Magnetic parameter$\left(= \sigma B_0{}^2 r_0/\rho_f u_\infty\right)$
P	Conjugate heat transfer parameter $\left(= k_f/k_c \ln(r_o/r_i)\, Re^{1/2}\right)$
Pr	Prandtl number$(= \nu_f/\alpha_f)$
r_i,r_0	inner and outer radii of the hollow cylinder (m)
Re	Reynolds number$(= u_\infty l/\nu_f)$
Ri	Richardson number$(= Gr/Re^2)$
T	temperature of the nanofluid (K)
$T_w(X)$	wall temperature (K)
u,v	velocities in x and r directions, respectively ($m\ s^{-1}$)
x,r	coordinates in axial and radial directions, respectively (m)

Greek Symbols

β	thermal expansion coefficient (K^{-1})
ε	porosity
η	similarity variable
λ	transverse curvature $\left(= 2\xi/Re_x^{1/2}\right)$
ζ	dimensionlessstreamwise coordinate $(= x/r_o)$
θ	dimensionless temperature
μ	dynamic viscosity ($kg\ m^{-1}\ s^{-1}$)
ν	kinematic viscosity ($m^2 s^{-1}$)
ρ	Density ($kg\ m^{-3}$)
σ	electric conductivity ($s^3\ A^2\ m^{-2}\ kg^{-1}$)
φ	nanoparticle volume fraction
ψ	streamline function $\left(= r_o(\nu_f u_\infty x)^{1/2} f(\xi,\eta)\right)$

Subscripts

F	fluid
Nf	Nanofluid
S	solid
∞	ambient

They found dual feasible solutions for the governing boundary layer equations. Kuznetsov and Nield [12] presented an analytical solution to investigate onset of convection in a horizontal layer of a porous medium saturated by a nanofluid. Darcy's law was used in the mathematical formulation for the porous layer.

Rosca et al. [13] used non-Darcy model to study mixed convection from a horizontal plate embedded in a nanofluid saturated by porous media. They also presented a correlation among reduced Nusselt number, nanoparticle volume fraction, inertia parameter and mixed convection parameter.

Some investigations have been dedicated to the hydrodynamic and thermal behavior of the nanofluid in porous media.

However, very few studies have been devoted to conjugate mixed convection of nanofluid flowing through porous media in presence of magnetic field. As such, the main objective of this research is to study the effects of pertinent dimensionless groups such as solid volume fraction parameter, conjugate heat transfer parameter, the porous medium parameter, the mixed convection parameter and the magnetic parameter on the thermal performance of flow and heat transfer characteristics.

BASIC EQUATIONS

Consider the laminar, steady, conjugate MHD-mixed convection of nanofluid about a vertical slender hollow cylinder embedded in a porous medium. The inside surface of the hollow cylinder is maintained at a constant temperature T_0, more than ambient temperature T_∞. In the formulation, $u_\infty$is the ambient nanofluid velocity, r_i and r_o are inner and outer radius of the circular cylinder, respectively and L is cylinder length. Figure 1 shows two-dimensional schematic geometry of the considered problem.

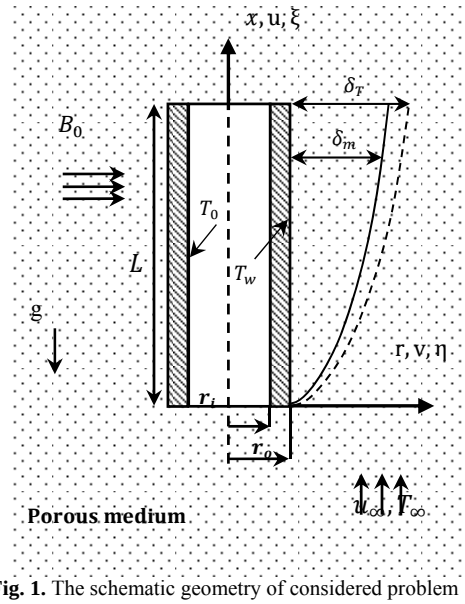


Fig. 1. The schematic geometry of considered problem

As seen in the Figure, the magnetic and gravitational forces are exerted in the horizontal and vertical directions, respectively.

Except for the preheater and furnace walls that are isothermal, other walls considered to be adiabatic. The

nanofluid is assumed to be incompressible and also thermophysical properties of the base fluid and nanoparticles are assumed to be constant listed in Table 1.

The buoyancy effects on momentum transfer are taken into account through the Boussinesq approximation.

Table 1
Thermophysical properties of the working fluid and the nano particle.

Physical properties	Fluid phase (water)	Nano particle (Cu)
C_p(J/kg K)	4179	385
ρ(kg/m^3)	997.1	8933
κ(W/m K)	0.613	400
$\alpha \times 10^7$(m^2/s)	1.47	1163.1
$\beta \times 10^5$(K^{-1})	21	1.67

Once the above assumptions are applied to the conservation equations of mass, momentum, and energy, set of governing equations is as follows:

$$\frac{\partial(\mathrm{ru})}{\partial \mathrm{x}} + \frac{\partial(\mathrm{rv})}{\partial \mathrm{r}} = 0 \tag{1}$$

$$\frac{1}{\epsilon^2}\left(\mathrm{u}\frac{\partial \mathrm{u}}{\partial \mathrm{x}} + \mathrm{v}\frac{\partial \mathrm{u}}{\partial \mathrm{r}}\right) = \frac{1}{\epsilon}\left(\frac{\nu_{\mathrm{nf}}}{\mathrm{r}}\right)\frac{\partial}{\partial \mathrm{r}}\left(\mathrm{r}\frac{\partial \mathrm{u}}{\partial \mathrm{r}}\right) + \frac{(\rho\beta)_{\mathrm{nf}}}{\rho_{\mathrm{nf}}} \times g(\mathrm{T} - \mathrm{T}_\infty) - \frac{\nu_{\mathrm{nf}}}{\mathrm{K}}(\mathrm{u} - \mathrm{u}_\infty) - \mathrm{F}(\mathrm{u}^2 - \mathrm{u}_\infty^2) - \frac{\sigma}{\rho_{\mathrm{nf}}}\mathrm{B}_0^2\,(\mathrm{u} - \mathrm{u}_\infty) \tag{2}$$

$$\mathrm{u}\frac{\partial \mathrm{T}}{\partial \mathrm{x}} + \mathrm{v}\frac{\partial \mathrm{T}}{\partial \mathrm{r}} = \frac{\mathrm{k}_{\mathrm{nf}}}{(\rho \mathrm{C}_\mathrm{p})_{\mathrm{nf}}}\frac{1}{\mathrm{r}}\frac{\partial}{\partial \mathrm{r}}\left(\mathrm{r}\frac{\partial \mathrm{T}}{\partial \mathrm{r}}\right) \tag{3}$$

Where u and v are the velocity components in x and r directions, respectively (see figure 1). T is the local temperature in the nanofluid, g is the acceleration due to gravity, K is permeability, F is inertia coefficient of the porous medium , σ is the electric conductivity and is B_0 magnetic field strength. In addition, the kinematic viscosity ν_{nf}, the dynamic viscosity μ_{nf}, the thermal conductivity k_{nf}, the density ρ_{nf} and the heat capacity $(\rho C_p)_{nf}$ of the nanofluid are given by:

$$\nu_{\mathrm{nf}} = \frac{\mu_{\mathrm{nf}}}{\rho_{\mathrm{nf}}}, \mu_{\mathrm{nf}} = \frac{\mu_{\mathrm{f}}}{(1-\varphi)^{2.5}}, \frac{\mathrm{k}_{\mathrm{nf}}}{\mathrm{k}_{\mathrm{f}}} = \frac{(2\mathrm{k}_{\mathrm{f}}+\mathrm{k}_{\mathrm{s}})-2\varphi(\mathrm{k}_{\mathrm{f}}-\mathrm{k}_{\mathrm{s}})}{(2\mathrm{k}_{\mathrm{f}}+\mathrm{k}_{\mathrm{s}})+\varphi(\mathrm{k}_{\mathrm{f}}-\mathrm{k}_{\mathrm{s}})},$$
$$\rho_{\mathrm{nf}} = (1-\varphi)\rho_{\mathrm{f}} + \varphi\rho_{\mathrm{s}},$$
$$(\rho C_{\mathrm{p}})_{\mathrm{nf}} = (1-\varphi)(\rho C_{\mathrm{p}})_{\mathrm{f}} + \varphi(\rho C_p)_{\mathrm{s}}$$
$$(\rho\beta)_{\mathrm{nf}} = (1-\varphi)\rho_{\mathrm{f}}\beta_{\mathrm{f}} + \varphi\rho_{\mathrm{s}}\beta_{\mathrm{s}} \tag{4}$$

Where φ is the solid volume fraction, β is the thermal expansion coefficient, ρ is density and subscripts f, s and nf denote fluid, solid and nanofluid, respectively. It is assumed that the thermal dispersion effect is minimal when the thermal diffusivity of the porous matrix is of the same order of magnitude as that of the working fluid [7].

The appropriate boundary conditions can be written as:

$$\begin{aligned} &\mathrm{r} = \mathrm{r}_\mathrm{o};\ \ \mathrm{u} = \mathrm{v} = 0,\ \ \mathrm{T} = \mathrm{T}_\mathrm{w}(\mathrm{x}) \\ &\mathrm{r} \to \infty;\ \ \mathrm{u} \to \mathrm{u}_\infty,\qquad \mathrm{T} \to \mathrm{T}_\infty \end{aligned} \tag{5}$$

Since the outer radius of the hollow cylinder, r_o, is assumed to be small, compared with its length, L, the axial conduction term in the heat conduction equation of the cylinder can be neglected [7, 14, 15] hence, one-dimensional heat conduction within the wall is supposed. $T_w(x)$ is temperature distribution of the outer cylinder surface, which should be determined as a boundary condition for thermal boundary layer equation. The governing equation for the temperature profile in relation to radial direction of the hollow cylinder is:

$$\frac{1}{\mathrm{r}}\frac{\partial}{\partial \mathrm{r}}\left(\mathrm{r}\frac{\partial \mathrm{T}}{\partial \mathrm{r}}\right)_{\mathrm{c}} = 0;\ 0 \le \mathrm{x} \le \mathrm{L}\ ;\ \mathrm{r}_\mathrm{i} < \mathrm{r} < \mathrm{r}_\mathrm{o} \tag{6}$$

The boundary conditions for the wall of the cylinder are given:

$$\text{At}\quad \mathrm{r} = \mathrm{r}_\mathrm{i}\ ,\ \mathrm{T}_\mathrm{i} = \mathrm{T}_0 \tag{7}$$

At the interface

$$\mathrm{r} = \mathrm{r}_\mathrm{o},\ \mathrm{T}_\mathrm{w} = \mathrm{T}(\mathrm{x}, \mathrm{r}_\mathrm{o}):\ -\mathrm{k}_\mathrm{c}\left.\frac{\mathrm{dT}}{\mathrm{dr}}\right|_{\mathrm{c}} = -\mathrm{k}_{\mathrm{nf}}\left.\frac{\partial \mathrm{T}(\mathrm{x},\mathrm{r}_\mathrm{o})}{\mathrm{dr}}\right|_{\mathrm{nf}} \tag{8}$$

Where k_c and k_{nf} are the thermal conductivity of the cylinder and the nanofluid, respectively. The boundary conditions given in equation 8 state the physical requirements that the temperature, heat fluxes of the cylinder and the nanofluid must be continuous across the solid-nanofluid interface. The temperature distribution of the outer cylinder surface, T_w, is derived as:

$$\mathrm{T}_\mathrm{w} = \mathrm{T}(\mathrm{x}, \mathrm{r}_\mathrm{o}) = \mathrm{r}_\mathrm{o}\frac{\mathrm{k}_{\mathrm{nf}}}{\mathrm{k}_\mathrm{c}}\ln\left(\frac{\mathrm{r}_\mathrm{o}}{\mathrm{r}_\mathrm{i}}\right)\frac{\partial \mathrm{T}(\mathrm{x}, \mathrm{r}_\mathrm{o})}{\partial \mathrm{r}} + \mathrm{T}_0 \tag{9}$$

Following Chang [7], we look for similarity solutions of equations (1-3) subject to the boundary conditions (5) of the following form:

$$\xi = \frac{\mathrm{x}}{\mathrm{r}_\mathrm{o}},\ \eta = \frac{1}{2\mathrm{x}}\mathrm{Re}_\mathrm{x}^{1/2}\left(\frac{\mathrm{r}^2 - \mathrm{r}_\mathrm{o}^2}{\mathrm{r}_\mathrm{o}}\right),\quad \theta = \frac{\mathrm{T} - \mathrm{T}_\infty}{\mathrm{T}_\mathrm{w} - \mathrm{T}_\infty},$$
$$\psi(\mathrm{x}, \mathrm{r}) = \mathrm{r}_\mathrm{o}(\nu_\mathrm{f}\mathrm{u}_\infty \mathrm{x})^{1/2} f(\xi, \eta) \tag{10}$$

Where the dimensionless variables ζ,ψ,η,θ and $\mathrm{Re}_\mathrm{x} = \mathrm{u}_\infty \mathrm{x}/\nu_\mathrm{f}$ are streamwise coordinate, free stream function, similarity variable, temperature and local Reynolds number, respectively. It is worth mentioning that the stream function satisfies the continuity equation (equation 1) hence, the velocity components can be defined:

$$u = \frac{1}{r}\left(\frac{\partial\psi}{\partial r}\right) = u_\infty f', \quad v = -\frac{1}{r}\left(\frac{\partial\psi}{\partial x}\right) = \frac{r_o}{r}\left(\frac{\nu_f u_\infty}{x}\right)^{1/2}\left[\frac{\eta}{2}f' - \frac{1}{2}f - \xi\frac{\partial f}{\partial\xi}\right] \tag{11}$$

Substituting equation 10 into equations (2-3) lead to the following non-dimensional differential equations:

$$\frac{1}{\epsilon}\left(\frac{\nu_{nf}}{\nu_f}\right)[(1+\lambda\eta)f''' + \lambda f''] + \frac{1}{2\epsilon^2}ff'' + \left(\frac{\beta_{nf}}{\beta_f}\right)\mathrm{Ri}\,\xi\theta - \left(\frac{\nu_{nf}}{\nu_f}\right)k_1\,\xi(f'-1) - F^*\,\xi((f')^2-1) - \left(\frac{\rho_f}{\rho_{nf}}\right)\xi M(f'-1) = \frac{\xi}{\epsilon^2}\left(f'\frac{\partial f'}{\partial\xi} - f''\frac{\partial f}{\partial\xi}\right) \tag{12}$$

$$\frac{1}{\Pr}\left(\frac{k_{nf}/k_f}{(\rho C_p)_{nf}/(\rho C_p)_f}\right)[(1+\lambda\eta)\theta'' + \lambda\theta'] + \frac{1}{2}f\theta' = \xi\left(f'\frac{\partial\theta}{\partial\xi} - \theta'\frac{\partial f}{\partial\xi}\right) \tag{13}$$

Where the prime symbol denotes differentiation with respect to η. In addition, the ratios of the nanofluid/fluid properties, appearing in the governing equations, can be defined as follows:

$$\frac{\nu_{nf}}{\nu_f} = \frac{1}{(1-\varphi)^{2.5}[(1-\varphi)+\varphi\,\rho_s/\rho_f]}, \quad \frac{\rho_{nf}}{\rho_f} = (1-\varphi)+\varphi(\rho_s/\rho_f), \quad \frac{\beta_{nf}}{\beta_f} = \frac{(1-\varphi)+\varphi(\rho_s/\rho_f)(\beta_s/\beta_f)}{(1-\varphi)+\varphi(\rho_s/\rho_f)} \tag{14}$$

These coupled equations have been solved as for the following transformed boundary conditions:

$$\eta = 0;\ f + 2\xi\frac{\partial f}{\partial\xi} = 0,\ f' = 0,\ \theta - 1 = (k_{nf}/k_f)p\xi^{-1/2}\theta',\ \eta\to\infty;\ f' = 1,\ \theta = 0 \tag{15}$$

Where $p = \frac{k_f}{k_c}\ln\left(\frac{r_o}{r_i}\right)\mathrm{Re}^{1/2}$ is the conjugate heat transfer parameter. The limiting case of p = 0 is correspond to isothermal boundary condition for equation 15. As seen in equation 14, the thermal conductivity ratio, k_{nf}/k_f, as a function of φ, is appeared in thermal boundary condition as well as in energy equation, it means that solid volume fraction is very important in the cooling process of the heated hollow cylinder.The dimensionless groups appearing in the governing equations are defined as follows:

$$\Pr = \frac{\mu_f C_{p_f}}{k_f},\ ,\ \mathrm{Ri} = \frac{\mathrm{Gr}}{\mathrm{Re}^2},\ \mathrm{Gr} = \frac{g\beta_f(T_0-T_\infty)r_0^3}{\nu_f^2},\ \mathrm{Re} = \frac{u_\infty r_o}{\nu_f},\ \lambda = 2\left(\frac{\xi}{\mathrm{Re}}\right)^{1/2},\ k_1 = \frac{\nu_f r_o}{Ku_\infty},\ F^* = \mathrm{Fr}_o, \tag{16}$$

$$\mathrm{Mn} = \frac{\sigma {B_0}^2 r_0}{\rho_f u_\infty}$$

Where Pr, Ri, Gr, Re, λ, k_1, F*and Mn are the Prandtl number, the Richardson number, the Grashof number, the Reynolds number, the transverse curvature parameter, the porous medium parameter, the inertia parameter (Forchheimer parameter) and Magnetic parameter, respectively. The transverse curvature parameter can also be rewritten as $\lambda = \left(2\xi/\mathrm{Re}_x^{1/2}\right)$ and the dimensionless interfacial temperature distribution θ_w, is defined as follows [7]:

$$\theta_w = \frac{T_w - T_\infty}{T_0 - T_\infty} \tag{17}$$

The average of reduced skin Friction and reduced Nusselt number can be defined as follows:

$$\mu_{nf}/\mu_f\,\overline{f''} = \sum_{j=1}^{n}\mu_{nf}/\mu_f\,f''(\eta=0,\xi_j)/10,\quad -k_{nf}/k_f\,\overline{\theta'} = -\sum_{j=1}^{n}k_{nf}/k_f\,\theta'(\eta=0,\xi_j)/10,\quad 0\le\xi_j\le 1 \tag{18}$$

Where j=0, 1, 2, …, n=10.

NUMERICAL METHOD AND VALIDATION

The coupled nonlinear differential equations 9 and 10 are numerically solved subject to the boundary conditions Equation 11 by using differential quadrature method. The DQM is an alternative discretization technique in order to solve directly the differential equation of physical systems mathematically [16] which requires less computer memory and CPU time in comparison with finite difference method. The solution is obtained in the following four steps:

1. The third-order partial differential equation is converted in the second-order system by substitution $g = f'$.
2. According to DQ method, η and ξ direction discretized into N_η and N_ξ.In this study, $\eta_\infty = 16$, $N_\eta = 60$,$\xi_\infty = 1$ and $N_\xi = 12$.
3. Linearizing the resulting algebraic equation by Newton's method.
4. Solving the linear system.

To conserve space, the details of the solution procedure are not presented here (see [17-19]). The relative error tolerance on the residuals is 10^{-3} and the absolute error tolerance is 10^{-6}. In order to demonstrate the precision of the present numerical procedure, the reduced skin friction $f''(\eta=0,\xi)$ and the reduced Nusselt number $\theta'(\eta=0,\xi)$ for regular fluid ($\varphi = 0$) were compared with previously published works.

As shown in Tables 2 and 3, an excellent agreement exists between our computed results and ones published in literatures.

RESULTS AND DISCUSSION

The present work has been carried out to study the hydrodynamic and thermal behavior of conjugate mixed convection of a nanofluid around the vertical cylinder embedded in a porous medium. The remaining parameters are specified as follows:

Richardson number (or mixed convection parameter) Ri=0,1,5,15, nanoparticle volume fraction φ=0,0.05,0.1and 0.15, conjugated heat transfer parameter, P=0,0.1,0.2,0.3, Magnetic parameter Mn=0,0.1,0.5,1.0,porous medium parameter K_1=0.1,0.5,1.0 and 2.0, inertia parameter F*=0.1,0.5,1.0 and 2.0. Hence, all of the numerical computations are performed with Re = 250 [15], ε=0.98[15] and Pr=6.2 [20].

Table 2

Comparison of $f''(\eta = 0, \xi)$with $Pr = 0.7$, Ri $= 0.0$, $\epsilon = 0.98$, $k_1 = 0.0$, $F^* = 0.0$, $p = 0.0$, Mn $= 0$ for regular fluid ($\varphi = 0$).

ξ	Chen and Mucoglu [30]	Chang [7]	Takhar et. al. [29]	Aydin and Kaya [28]	Kaya [9]	Present results
0	1.3282	1.3280	1.3281	1.3261	1.3201	1.3282
1	1.9172	1.9133	1.9167	1.9134	1.8934	1.9175
2	2.3981	2.3900	2.3975	2.3902	2.3822	2.3989
3	2.8270	2.8159	-	2.8148	2.8098	2.8283
4	3.2235	3.2187	-	3.2162	3.2102	3.2252

Table 3

Comparison of $-\theta'(\eta = 0, \xi)$with $Pr = 0.7$, Ri $= 0.0$, $\epsilon = 0.98$, $k_1 = 0.0$, $F^* = 0.0$, $p = 0.0$,Mn $= 0$, for regular fluid ($\varphi = 0$).

ξ	Chen and Mucoglu [30]	Chang [7]	Takhar et. al. [29]	Aydin and Kaya [28]	Kaya [9]	Present results
0	0.5854	0.5852	0.5854	0.5846	0.5846	0.5853
1	0.8669	0.8658	0.8666	0.8599	0.8599	0.8670
2	1.0986	1.0940	1.0963	1.0918	1.0918	1.0974
3	1.3021	1.2982	-	1.2902	1.2902	1.3030
4	1.4921	1.4925	-	1.4898	1.4898	1.4933

Effect of Richardson number on interfacial temperature and nanofluid velocity and temperature within boundary layer are shown in Figure 2(a-c), respectively.The dimensionless number represents the importance of Buoyancy forces (caused by a temperature gradient) in relation to the external forced convection in many thermal energy problems.

Buoyancy forces can enhance the surface heat transfer rate when they assist the forced convection [21] since for assisting flow, the buoyancy force acts in the same direction as upward external forced. Hence, interfacial temperature drops with rising Ri and it could be observed in Figure 2a. Since these computations are carried in fixed Reynolds number (Re=250), increasing the Ri is correspond to increasing Buoyancy force (in the streamwise direction), which causes to move the nanofluid at an accelerated rate in the vicinity of the cylinder surface.

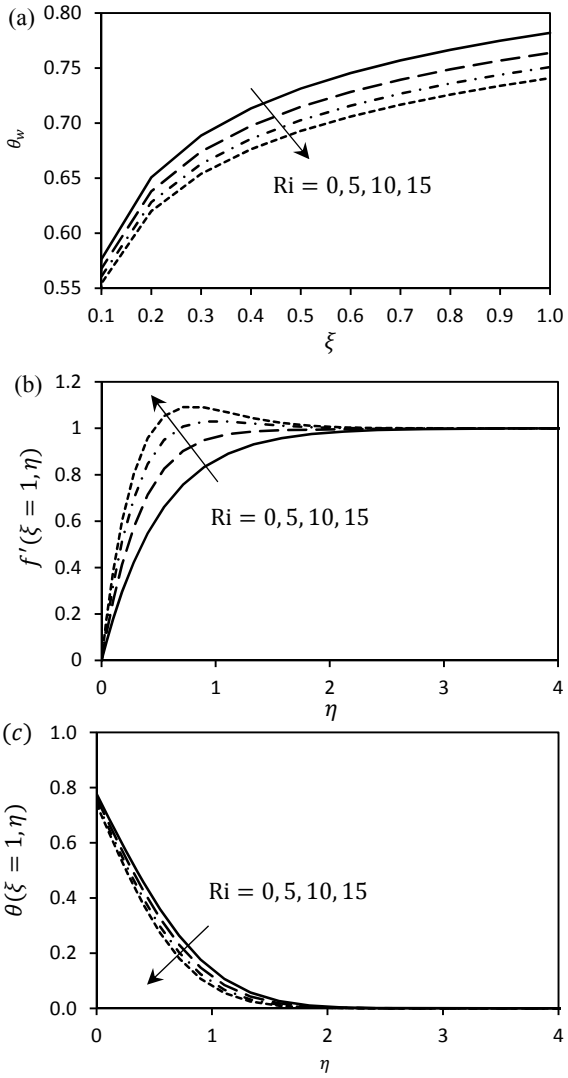


Fig. 2. Effect of Richardsonnumber Ri on dimensionless interfacial temperature θ_w (a), velocity $f'(\xi = 1, \eta)$ (b) and temperature $\theta(\xi = 1, \eta)$ (c) while $\varphi = 0.1$, p=0.2,Mn=0.5, k_1=1.0 and F*=1.0

Therefore, velocity profile is increased for large Ri in this location so an overshoot is formed in Figure 2b. In addition, it can be seen in Figure 2c, an increasing in the Richardson number lead to a sharp temperature gradient (at the surface of solid, $\eta = 0$) and the decrease in the thermal boundary layer thickness.

Note that the solid line corresponds to the case of pure forced convection (Ri = 0). Figures 3(a-c) display typical

the dimensionless interfacial temperature θ_W velocity $f'(\xi = 1, \eta)$ and temperature $\theta(\xi = 1, \eta)$ profile in boundary layer, respectively.

These profiles are for Cu–water nanofluid and different values of the nanoparticle parameter φ = 0, 0.05, 0.1 and 0.15 when $\epsilon = 0.98$, Ri=5, p=0.2, Mn=0.5, k_1=1 and F*=1.

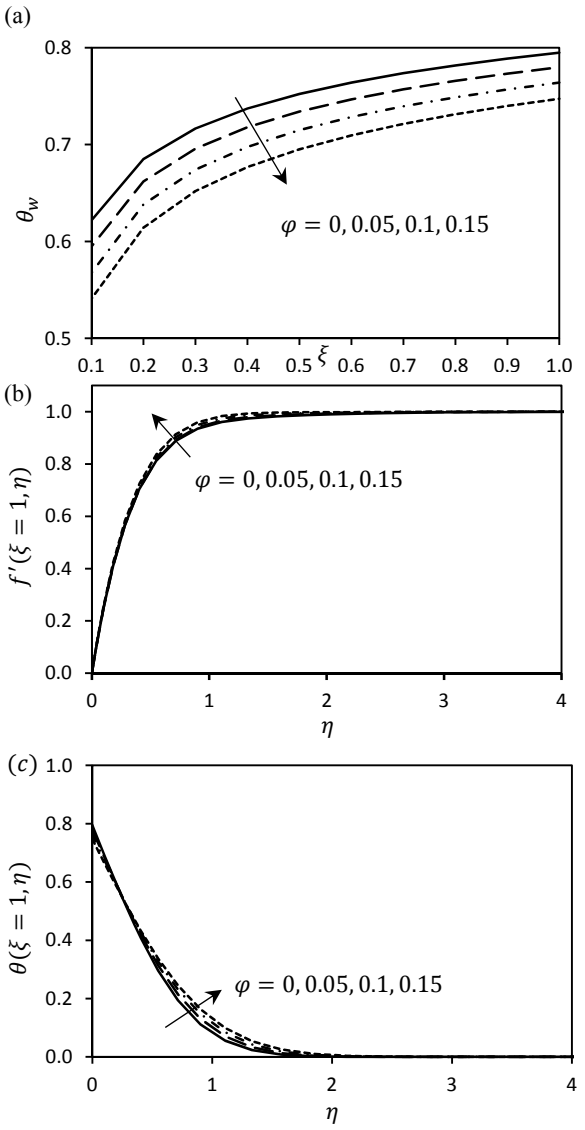


Fig. 3. Effect of solid volume fractionφ on dimensionless interfacial temperature θ_w (a), velocity $f'(\xi = 1, \eta)$ (b) and temperature $\theta(\xi = 1, \eta)$ (c) while Ri=5, p=0.2,Mn=0.5, k_1=1.0 and F*=1.0

It is seen from Figure 3a that the interfacial temperature is increasing function of nano particle volume fraction and these profiles increase monotonically with ξ for a given value of φ. From the physical point of view, the increases of the parameter φ leads to an increasing of the viscosity and thermal conductivity of the nanofluid (see equation 4). The momentum boundary layer thickness, vicinity the hollow cylinder surface, decreases with the increasing of the nanoparticle concentration parameter φ (see Figure 3b). As displayed in Figure 3c, the dimensionless temperature profiles are affected by increasing the nanoparticle concentration. Similar behaviors have been also reported by Grosan and Pop [20] for nanofluid flow past a vertical cylinder in the absence of porous media. The effects of conjugate heat transfer parameter p on the dimensionless wall temperature with Ri=5, φ=0.1, Mn=0.5, k_1=1.0 and F*=1.0 has shown in Figure 4a. The increasing of the conjugate heat transfer parameter decreases velocity and temperature gradients at the wall. A lower wall conductance k_c or larger cylinder thickness or higher convective cooling effect (due to greater k_f) increases the value of p causing greater temperature difference between the two surfaces of the cylinder. Thus the temperature of the cylinder-nanofluid interface is reduced when the temperature of the inner surface of the cylinder is kept constant.

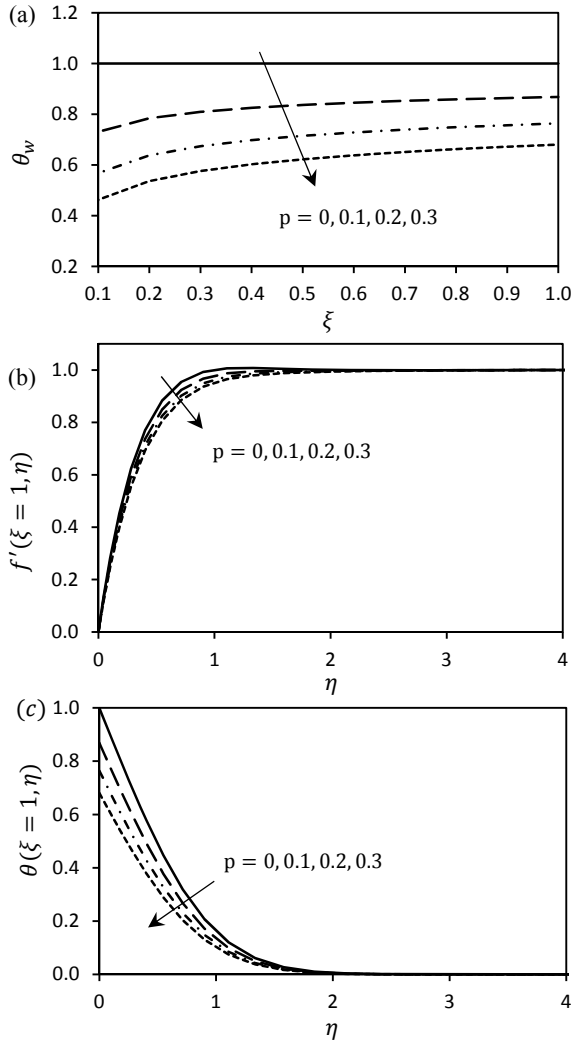
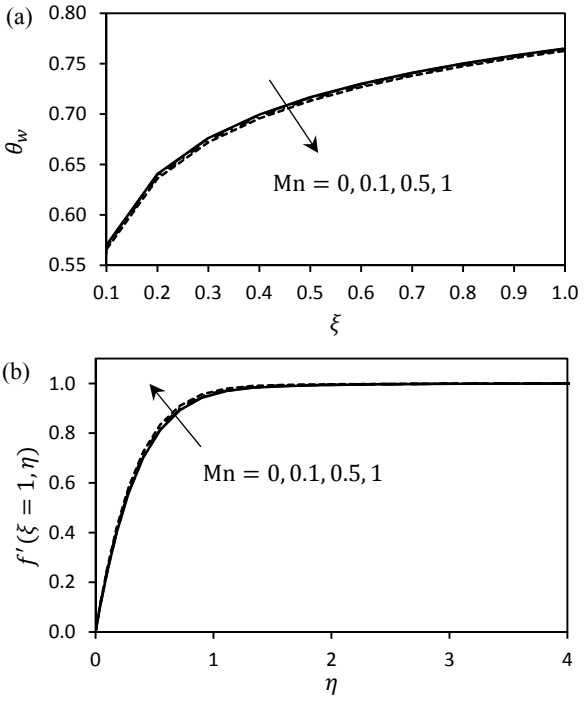


Fig. 4. Effect of conjugate heat transfer parameterp on dimensionless interfacial temperature θ_w (a), velocity $f'(\xi = 1, \eta)$ (b) and temperature $\theta(\xi = 1, \eta)$ (c) while Ri=5, φ=0.1, Mn=0.5, k_1=1.0 and F*=1.0

It is clearly observed, when p increases temperature profile at outer cylinder surface Figure 4a and in nanofluid (figure 4c) in boundary layer decrease. Hence, effect of buoyancy (assisting inertia force) and nanofluid velocity will decrease, as seen in Figure 4b. The solid lines and dashed lines in these figures indicate the skin friction factor corresponding to the cases of isothermal cylinder (p = 0) and non-isothermal cylinder (p > 0), respectively.The variations of the interfacial temperature, velocity and temperature of the nanofluid in boundary layer for different values of Magnetic parameter have been presented in Figure 5(a-c), respectively where Ri=5, φ=0.1, p=0.2, k_1=1.0 and F*=1.0. It can be seen from Figure 5a that the wall temperature increases monotonically with ξ and is decreasing function of Magnetic parameter. In addition, the momentum boundary layer thickness decreases by increasing of the Magnetic parameter Mn, while the thermal boundary layer thickness increases, as seen in Figure 5b and c, respectively. Methinks magnetic field is exerted on nanofluid as body force (as well as gravity force but in reverse direction) in order to move it along downstream with more velocity and it has a positive effect on cooling performance although it is not a remarkable one (as shown in Figure 5).In the Forchheimer–Brinkman-extended Darcy model, the axial pressure drop is represented by the sum of two terms; ($-\frac{dp}{dx} = \frac{\nu}{K}u + Fu^2$ [9, 22, 23]) in the right side of the equation the first term has a linear with the velocity (viscous contribution) and the second one is proportional to the square of the fluid velocity to account as the inertial of the fluid flow (inertial contribution) as it makes its way through the porous medium. In this section, the effects of these two parameters are discussed.



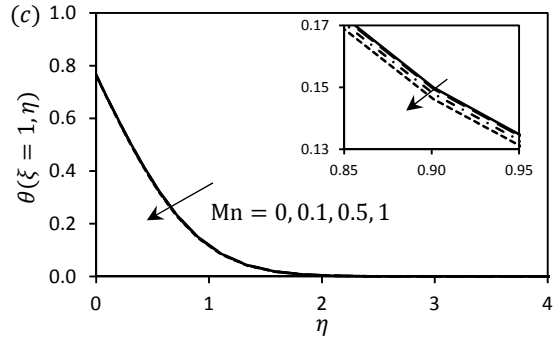


Fig. 5. Effect of Magnetic parameter Mn on dimensionless interfacial temperature θ_w (a), velocity $f'(\xi = 1, \eta)$ (b) and temperature $\theta(\xi = 1, \eta)$ (c) while Ri=5, $\varphi = 0.1$, p=0.2, k_1=1.0 and F*=1.0.

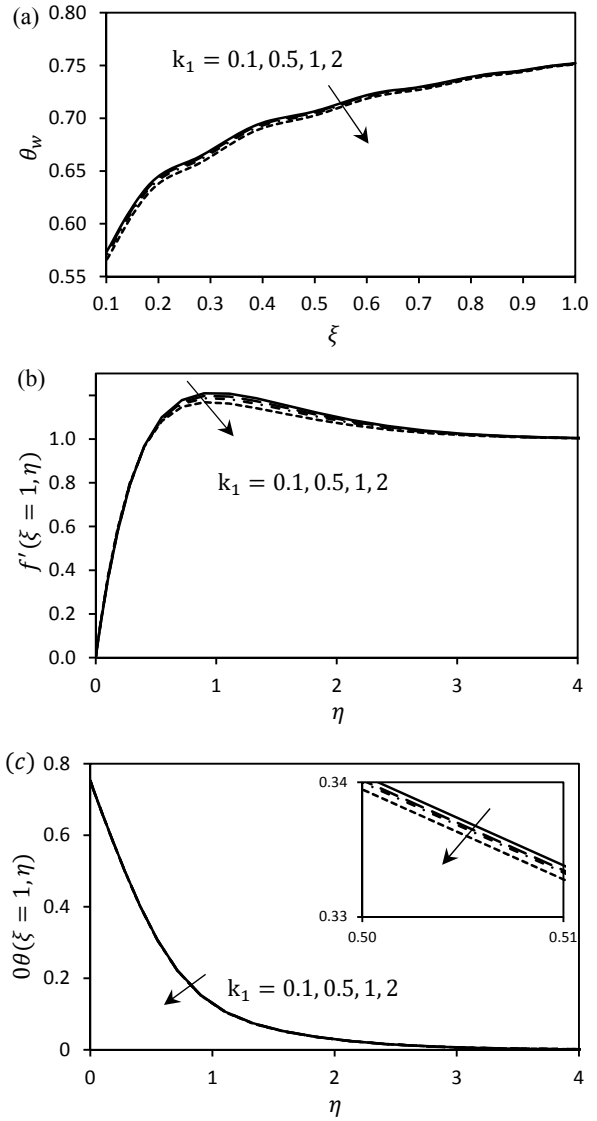
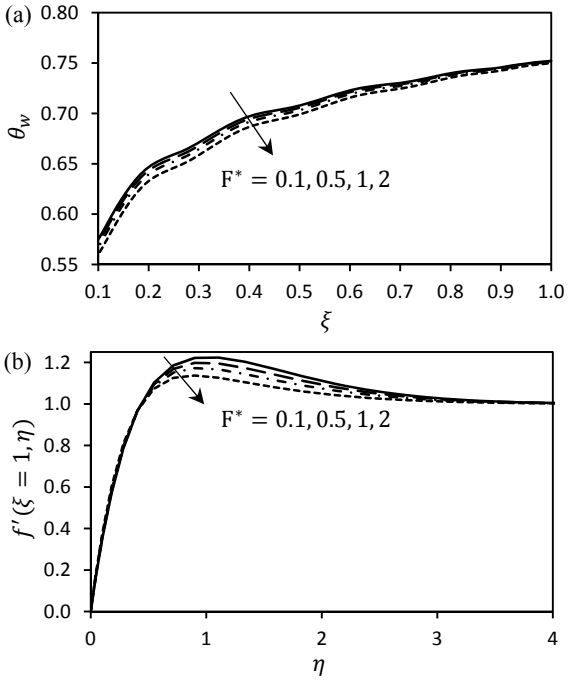


Fig. 6. Effect of porous medium parameterk_1 on dimensionless interfacial temperature θ_w (a), velocity $f'(\xi = 1, \eta)$ (b) and temperature $\theta(\xi = 1, \eta)$ (c) while Ri=15, φ=0.1, p=0.2, Mn=0.5 and F*=1.0

It is observed that the wall temperature increases by increasing the streamwise ξ. It is because of growing thermal boundary layer (which corresponds to growing thermal resistance) along the axis of the hollow cylinder. Hence, temperature profiles rise monotonically in this direction. In addition, this temperature decreases by increasing k_1 as shown in Figure 6a. Since the porous medium parameter is directly proportional to the fluid kinematic viscosity and inversely proportional to the permeability of the porous medium, velocity profiles decrease by increasing k_1. Also this type of resistive force acts to decelerate the motion of the fluid within the boundary layer. This is indeed observed in Figure 6b, where velocity clearly decreases as k_1 rises from 0.1 to 2. It seen from Figure 6c that increasing the value of the porous medium parameter causes to decrease temperature boundary layer.

The variations of the dimensionless interfacial temperature distributions as a function of ξ in the boundary layer are displayed in Figure 7a. It can be observed that as the value of ξ increases, the interfacial temperature rises, i.e. the interfacial temperature increases from the bottom of the cylinder towards the top of it. Figure 7b and c represent effects of the inertia parameter on velocity and temperature, respectively the fixed streamwise $\xi = 1$. The porous medium inertial parameter F^* provides a resistance to flow mechanism which causes the fluid to move at a slower rate and its temperature increases [24] since Forchheimer friction term is directly related to pressure drag inside the porous matrix. It seen in Figure 7b and c by increasing the value of the inertia parameter to decrease causes both velocity and temperature profile.



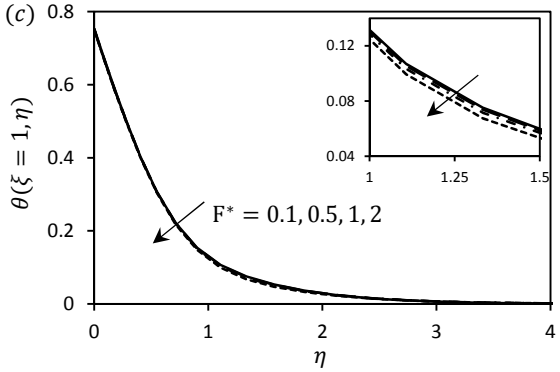


Fig. 7. Effect of Forchheimer parameter F^* on dimensionless interfacial temperature θ_w (a), velocity $f'(\xi = 1, \eta)$ (b) and temperature $\theta(\xi = 1, \eta)$ (c) while Ri=15, $\varphi = 0.1$, p=0.2, Mn=0.5 and k_1=1.0

Effects of average skin friction and average Nusselt number are also studied in this work. In order to save space, we have summarized and presented our computed results in tables. According to the mentioned explanation, it is clearly found that the average skin friction and average heat transfer increase as the values of φ, k_1, F^* increase. This trend not only occur on isothermal cylinder (p = 0), but also in the non-isothermal cylinder (p > 0). While these two parameters decrease by increasing conjugate heat transfer parameter p. These behaviors are obviously displayed in Tables 4, 5.

CONCLUSION

A numerical study of upward mixed convection of nanofluid (water/Cu) flow along vertical slender hollow cylinder embedded in porous media in presence of a transverse magnetic field has been carried out. The Non-Darcy's law was applied to the mathematical formulation for the high porosity porous media. Also similarity solution approach was used to transform the governing dimensional PDEs into non-dimensional PDEs then solved by using Differential Quadrature Method (DQM). The calculations are performed for different values of Richardson number, nanoparticle volume fraction, conjugate heat transfer, Magnetic, porous medium and inertia parameters. Our study shows that the skin friction and the Nusselt number could be significantly increased by Ri, φ, k_1 and F^*, while these parameters are decreased by increasing p,and Magnetic parameter has no notable effect on both of them.

Table 4

Values related to the reduced average skin friction $\mu_{nf}/\mu_f \overline{f''}$,$(0 \le \xi \le 1.0)$ for different values of the governing parameters when $\epsilon = 0.98$, $Pr = 6.2$, Ri=5, Mn $= 0.5$.

p	φ	$k_1 = \mathbf{0.1}$			$k_1 = \mathbf{0.5}$			$k_1 = \mathbf{1.0}$		
		F*			F*			F*		
		0.1	**0.5**	**1.0**	**0.1**	**0.5**	**1.0**	**0.1**	**0.5**	**1.0**
0	**0.05**	4.141	4.416	4.724	4.309	4.560	4.854	4.494	4.730	5.010
	0.10	4.380	4.724	5.106	4.543	4.870	5.237	4.735	5.044	5.395
	0.15	4.698	5.117	5.579	4.864	5.265	5.711	5.062	5.442	5.871
0.1	**0.05**	3.838	4.087	4.430	3.938	4.219	4.534	4.140	4.403	4.700
	0.10	3.999	4.364	4.775	4.170	4.524	4.916	4.379	4.711	5.084
	0.15	4.293	4.747	5.241	4.475	4.906	5.381	4.689	5.096	5.551
0.2	**0.05**	3.773	4.073	4.404	3.949	4.230	4.545	4.151	4.413	4.711
	0.10	4.003	4.377	4.786	4.182	4.535	4.927	4.390	4.722	5.094
	0.15	4.305	4.759	5.252	4.487	4.918	5.392	4.701	5.108	5.562

Table 5

Values related to the reduced average Nusselt number $-k_{nf}/k_f\ \bar{\theta}'$,$(0 \le \xi \le 1.0)$ for different values of the governing parameters $\epsilon = 0.98$, $Pr = 6.2$, Ri=5, Mn=0.5.

p	φ	$\mathbf{k_1}$**=0.1**			**k_1=0.5**			**k_1=1.0**		
		F*			F*			F*		
		0.1	**0.5**	**1.0**	**0.1**	**0.5**	**1.0**	**0.1**	**0.5**	**1.0**
0	**0.05**	1.061	1.081	1.100	1.069	1.089	1.107	1.080	1.098	1.115
	0.10	1.160	1.184	1.207	1.170	1.192	1.213	1.182	1.201	1.221
	0.15	1.268	1.295	1.321	1.278	1.303	1.327	1.289	1.312	1.334
0.1	**0.05**	0.869	0.895	0.924	0.875	0.893	0.912	0.887	0.903	0.920
	0.10	0.946	0.968	0.992	0.955	0.977	0.999	0.967	0.987	1.007
	0.15	1.030	1.060	1.087	1.042	1.068	1.093	1.054	1.077	1.100
0.2	**0.05**	0.869	0.891	0.911	0.882	0.901	0.920	0.894	0.911	0.927
	0.10	0.950	0.976	1.000	0.963	0.986	1.008	0.975	0.995	1.015
	0.15	1.039	1.069	1.096	1.051	1.077	1.102	1.063	1.086	1.110

REFERENCES

[1] D. A. Nield, A. Bejan, Convection in Porous Media: Springer (2006).

[2] K. Vafai, Handbook of Porous Media, Second Edition: Taylor & Francis (2010).

[3] K. Vafai, Porous Media: Applications in Biological Systems and Biotechnology: Taylor & Francis (2010).

[4] D. B. Ingham, I. Pop, Convective Heat Transfer: Mathematical and Computational Modelling of Viscous Fluids and Porous Media: Elsevier Science (2001).

[5] D. B. Ingham and I. Pop, Transport Phenomena in Porous Media III: Elsevier Science (2005).

[6] P. Vadász, Emerging Topics in Heat and Mass Transfer in Porous Media: From Bioengineering and Microelectronics to Nanotechnology: Springer Science+Business Media B.V(2008).

[7] C.-L.Chang: Buoyancy and wall conduction effects on forced convection of micropolar fluid flow along a vertical slender hollow circular cylinder, International Journal of Heat and Mass Transfer 49 (2006) 4932-4942.

[8] A. Kaya: The effect of conjugate heat transfer on MHD mixed convection about a vertical slender hollow cylinder, Communications in Nonlinear Science and Numerical Simulation 16 (2011) 1905-1916.

[9] S. U. S. Choi, Z. G. Zhang, W. Yu, F. E. Lockwood, ,E. A. Grulke: Anomalous thermal conductivityenhancement in nanotube suspensions, Applied Physics Letters 79 (2001) 2252-2254.

[10] S. Ahmad, I. Pop: Mixed convection boundary layer flow from a vertical flat plate embedded in a porous medium filled with nanofluids, International Communications in Heat and Mass Transfer 37 (2010) 987-991.

[11] A. V. Kuznetsov, D. A. Nield: Effect of Local Thermal Non-equilibrium on the Onset of Convection in a Porous Medium Layer Saturated by a Nanofluid, Transport in Porous Media 83(2010)425

-436.

[12] A. V. Rosca, N. C. Rosca, T. Grosan, I. Pop: Non-Darcy mixed convection from a horizontal plate embedded in a nanofluid saturated porous media, International Communications in Heat and Mass Transfer 39 (2012) 1080-1085.

[13] T.-Y. Na: Effect of wall conduction on natural convection over a vertical slender hollow circular cylinder, Applied Scientific Research 54 (1995) 39-50.

[14] A. Kaya: Effects of buoyancy and conjugate heat transfer on non-Darcy mixed convection about a vertical slender hollow cylinder embedded in a porous medium with high porosity, International Journal of Heat and Mass Transfer 54 (2011) 818.

[15] H. Rahideh, P. Malekzadeh, M. R. Golbahar Haghighi: Non-Fourier Heat Conduction Analysis with Temperature-Dependent Thermal Conductivity, ISRN Mechanical Engineering 2011 (2011) 4-6.

[16] P. Malekzadeh, H. Rahideh, A. R. Setoodeh: Optimization of non-symmetric convective–radiative annular fins by differential quadrature method, Energy Conversion and Management 48 (2007) 1671-1677.

[17] P. Malekzadeh, H. Rahideh: Two-dimensional nonlinear transient heat transfer analysis of variable section pin fins, Energy Conversion and Management 50 (2009) 916-922.

[18] H. Rahideh, P. Malekzadeh, M. R. Golbahar Haghighi: Heat conduction analysis of multi-layered FGMs considering the finite heat wave speed, Energy Conversion and Management 55 (2012) 14-19.

[19] T. Grosan, I. Pop: Axisymmetric mixed convection boundary layer flow past a vertical cylinder in a nanofluid, International Journal of Heat and Mass Transfer 54 (2011) 3139-3145.

[20] H. S. Takhar, A. J. Chamkha, G. Nath: Combined heat and mass transfer along a vertical moving cylinder with a free stream, Heat and Mass Transfer 36 (2000) 237-246.

[21] C. Cheng-Long: Numerical simulation of micropolar fluid flow along a flat plate with wall conduction and buoyancy effects, Journal of Physics D: Applied Physics 39 (2006)1132.

[22] M. A. Chen TS: Bouyancy Effects on Forced Convection Along a Vertical Cylinder, ASME. J. Heat Transfer 97 (1975) 198-203.

[23] O. Aydın, A. Kaya: Mixed convection of a viscous dissipating fluid about a vertical flat plate, Applied Mathematical Modelling 31 (2007) 843-853.

[24] K. Vafai, C. L. Tien: Boundary and inertia effects on flow and heat transfer in porous media, International Journal of Heat and Mass Transfer 24 (1981)195-203.

[25] K. A. J. Al-Farhany: Numerical investigations of heat and mass transfer in a saturated porous cavity with Soret and Dufour effects (2012) 64-65.

[26] A. Kaya: Effects of buoyancy and conjugate heat transfer on non-Darcy mixed convection about a vertical slender hollow cylinder embedded in a porous medium with high porosity, International Journal of Heat and Mass Transfer 54 (2011) 818-825.

[27] A. J. Chamkha: Non-similar solutions for heat and mass transfer by hydro-magnetic mixed convection flow over a plate in porous media with surface suction or injection, International Journal of Numerical Methods for Heat & Fluid Flow 10 (2000) 142 - 163.